J Mol Model (2011) 17:1973–1984
DOI 10.1007/s00894-010-0895-1

ORIGINAL PAPER

Computational synthesis of hydrogenated fullerenes from C_{60} to $C_{60}H_{60}$

Elena F. Sheka

Received: 17 August 2010 / Accepted: 31 October 2010 / Published online: 3 December 2010

Abstract Hydrogenation from C_{60} to $C_{60}H_{60}$ was studied by an unrestricted broken spin symmetry Hartree–Fock approach implemented in semiempirical codes based on the AM1 technique. The calculations focused on the successive addition of hydrogen molecules to the fullerene cage following the identification of the cage target atoms by calculating the highest atomic chemical susceptibility at each step. The results obtained are analyzed from energy, symmetry, and composition perspectives.

Keywords Hydrogenated fullerene C_{60} · Quantum chemistry · Unrestricted broken symmetry approach · Atomic chemical susceptibility · Computational synthesis

Introduction

The effectively unpaired electron concept, which relates to the chemical susceptibility of fullerene atoms [1–3], lays the foundation for the stepwise computational synthesis of the hydrogenated derivatives of fullerene C_{60} that is performed in the current study. The methodology used here, which utilizes an unrestricted broken symmetry HF (UBS HF) SCF semiempirical approach (UBS HF version of the AM1 technique of the CLUSTER-Z1 codes), was originally applied to fluorination from C_{60} to $C_{60}F_{60}$ [4], but it is used here for hydrogenation from C_{60} to $C_{60}H_{60}$. The calculations focus on the successive addition of hydrogen molecules to the fullerene cage. A complete family of species of formula $C_{60}H_{2k}$ k=(1, ..., 30) was produced. To avoid the manyfold isomerism problem (as discussed in detail in [4]) of the enormous number of structural isomers that are possible for, say, $C_{60}H_{36}$ (~6×10^{14}) and $C_{60}H_{48}$ (~2×10^{10}) [5], the preferred binding sites for successive additions are selected according to the largest value of the atomic chemical susceptibility (ACS), as quantified by the effectively unpaired electron fraction N_{DA} on the atom considered, A [2, 3]. As shown, any addition of a hydrogen molecule causes a noticeable change in the N_{DA} distribution over the C_{60} cage atoms. Consequently, the synthesis was performed as a series of predicted steps. The reaction starts at the pair of fullerene C_{60} atoms with the biggest N_{DA} values. The atoms usually form a short bond within one of six identical naphthalene-core fragments. When the first adduct ($C_{60}H_2$) is formed, the reaction proceeds at a new pair of fullerene cage atoms that now have the highest N_{DA} values, thus resulting in the formation of the $C_{60}H_4$ hydride. A new N_{DA} map is then generated that reveals the sites for the next addition step, and so on. Thirty hydrogenation steps from C_{60} to $C_{60}H_{60}$ were performed according to this methodology. The results obtained are analyzed from energy, symmetry, and composition viewpoints, and are compared with experimental data where possible.

Computational methodology

The hydrogenation of C_{60} was one of the first reactions of fullerenes to be considered computationally. The list of publications on this subject is rather long (see a detailed review of papers published by the beginning of 1994 in [6], some later papers [7–10], and a collection of works by Clare and Kepert [11–17]). Taken together, these calculations cover practically all of the available computational schemes applied to the species. However, the differences between

E. F. Sheka (✉)
Peoples' Friendship University of Russia,
117197, Moscow, Russia
e-mail: sheka@icp.ac.ru

the results generated by different techniques was not the reason for the multitude of investigations performed on this topic. The main issue was the derivation of structural models of hydrides, considering the manyfold isomerism problem. Experimental findings that could help to solve the problem have been rather scarce until now, and can be summarized as follows: (1) polyaddition hydrides are abundant among the products formed; (2) the hydrides are characterized by even numbers of hydrogen atoms; (3) the appearance of isomerism is limited to just a few isomers [10, 18, 19]. Therefore, in order to be practically useful, simulations had to appropriately select one or a few polyhydride isomers. The only clear evidence for how to achieve this goal concerns the addition of a pair of hydrogen atoms at each successive step. This occurs in both types of hydrogenation: molecular hydrogenation, which is characteristic of the Birch reduction of C_{60} [20], and atomic radical reactions, which occur in the transfer hydrogenation of C_{60} with dihydroanthracene [21] or in the hydrogenation of fullerite at elevated temperatures and hydrogen pressures [22].

When constructing the structural models needed for such calculations, the first question is: are the first and subsequent pairs of hydrogen atoms accommodated on the fullerene cage via 1,2 addition (suitable for the addition of both a hydrogen molecule and a pair of separated hydrogen atoms) or via 1,4 addition (suitable only for separated atoms)? The differences in energy were attributed to the result that only 1,2 addition does not disrupt the remaining polyene structure of the cage, whereas one double (short) bond is moved to a five-membered ring in the case of 1,4 addition. A thorough study [23] showed the preference of hydrogen for 1,2 addition, and made it possible to consider successive steps as individual 1,2 additions of a hydrogen molecule to the fullerene cage.

There are also two other questions: how does the addition of each hydrogen pair occur, and what reasons govern the selection of a single isomer? In terms of the manner of the successive additions, a conjectured contiguous route to the formation of polyhydrides was accepted [9, 19]. The main suggestion for selecting isomers was to pick isomers of high symmetry followed by the further selection of the species with the least total energy. Originating with the first experiment to produce $C_{60}H_{36}$, where T_h symmetry was assumed for the species [18], this high-symmetry selection was supported by the structural characterization of $C_{60}H_{18}$ [19], which allowed a C_{3v} symmetry crown structure to be quite reliably established. Afterwards, this idea was commonly applied to all calculations relating to polyhydrides, particularly $C_{60}H_{36}$ [7, 8, 13–17].

All computations make use of closed-shell restricted single-determinant computational schemes; both Hartree-Fock and DFT. When applied to the C_{60} fullerene cage, this means accepting completely covalent bonding of the molecule's odd electrons. The latter are considered classic π electrons that are typical of the benzene molecule. However, this is not the case for the C_{60} molecule itself [1–3] and its low-k fluorides [4], due to a weaker interaction between the odd electrons of the cage caused by increased C–C bond lengths in comparison with the benzene molecule. This feature is clearly justified by the fact that the energy of the species calculated in the single-determinant open-shell unrestricted approximation is markedly lower than that of the closed-shell scheme. This finding is of great importance, and leads to a problem with the general applicability of single-determinant calculation schemes. As is known, weakly interacting electrons should be considered from the viewpoint of many-electron configurational interaction (CI) schemes, while even the unrestricted open-shell approximation—which yields the most accurate energies among single-determinant schemes—is not related to pure spin states and is spin contaminated. However, exact CI calculations of big molecules like fullerene C_{60} are not feasible, so unrestricted single-determinant schemes are currently the only alternative. Fortunately, Noodleman [24] showed a straightforward way to connect the unrestricted single-determinant spin-contaminated solutions with the pure-spin ones, thus suggesting a practical unrestricted broken spin symmetry (UBS) approach. On the other hand, it was proposed that the solution spin contamination could be quantified based on the number of effectively unpaired electrons [25, 26]. As was shown later [2, 3], within the framework of the UBS HF approach, the total number of effectively unpaired electrons N_D provides a numeric description of the molecule's chemical susceptibility, while the fraction on each atom N_{DA} furnishes the atomic chemical susceptibility (ACS). In contrast to HF theory, DFT does not suggest such characteristics, due to problems with total spin [27, 28]. This is why the UBS DFT approach is mainly limited only by the determination of the difference in pure-spin state energies (magnetic coupling constant) within the framework of complicated schemes [29, 30].

As shown in the current study, the UBS HF approach—similar to the restricted HF approach used in [23]—reveals the preference of hydrogen atoms for 1,2 addition rather than 1,4 addition. This allows us to consider all successive steps of hydrogenation as individual 1,2-addition steps. In terms of both the conjectured contiguous route and the high symmetry criterion for isomer selection, our approach does not need any of these assumptions, since changing the ACS (N_{DA}) map after each addition creates a definite algorithm for H_2 addition in accordance with the highest N_{DA} values. Moreover, the validity of these two assumptions can be readily checked as the computational synthesis is performed.

All hydrogen atoms are bound to the exterior surface of the cage. The small size of the hydrogen atom also makes it

favorable for them to penetrate inside the cage too. As shown earlier [31], having some hydrogens inside and others outside the cage promotes cage stabilization, reducing the cage strain produced by hydrogenation. However, taking into account the empirically established parallelism on the one hand, and the differences on the other, between fluorinated and hydrogenated polyderivatives of C_{60}, the computations presented in this paper aimed to not only pinpoint the series of hydrides formed, but also to elucidate the reasons for the behaviors of these two families. Since only fluorides with their fluorines on the outside of the fullerene cage are available for comparison, only hydrides with their hydrogens on the outside of the cage are considered in this paper.

Algorithm of the computational synthesis of C_{60} hydrides

An analysis of the odd-electron-enhanced chemical activity of the C_{60} molecule highlights its "chemical portrait," as shown by the ACS distribution (N_{DA} map) over the atoms of the molecule [2, 3]. According to the latter, the molecule consists of six identical naphthalene-core fragments forming a $6 \times C_{10}$ configuration. Using different colors for atoms with different ACSs, Fig. 1 visualizes the portrait in the form of either the structure of the molecule (Fig. 1a) or its projection on a Schlegel diagram (Fig. 1b), whereas the corresponding numerical ACS distribution is given in Fig. 1c. The colors in the structure of the molecule and the Schlegel diagram correspond to particular atom groups in the output file (as defined by the key in the top left of Fig. 1b). The values of N_{DA} in Fig. 1c are plotted from the highest to the lowest in a Z→A manner, so the numbering does not correspond to that shown in Fig. 1b. Figure 1c shows that there are five groups of atoms that each consist of six identical pairs, as shown in Fig. 1a and b by the different colors. The marginal position of group 5 on the ACS map makes it possible to ignore a small variation in N_{DA} within this group.

According to the figure, the initial step in any addition reaction involving fullerene C_{60} must concern atoms of group 1, which are characterized by the highest N_{DA} values. Any one of the six pairs in this atom group can be involved in the start of the reaction, where one hydrogen molecule attaches to the fullerene cage computationally, just like any other atomic or molecular addition. When the first hydride $C_{60}H_2$ is formed, the map of its fullerene cage exhibits different atoms with the highest N_{DA} values, and the next reaction step will involve these atoms. After the formation of $C_{60}H_4$, its N_{DA} map reveals the sites for the next addition step, and so on. When there are quite a few atoms with the highest N_{DA} value, a few isomers are considered and an additional analysis of the formed isomers based on the total energy is performed in order to choose the isomer with the least energy. Using this methodology, a complete list of fluorinated fullerenes $C_{60}F_{2k}$ were synthesized in [4]. By repeating the procedure described in that work, a complete list of C_{60} hydrides was obtained in the current study. The suggested algorithm for the computational synthesis of the family of fullerene hydrides can be directly attributed to the actual experimental hydrogenation of C_{60} in gaseous hydrogen.

Results and discussion

C_{60} hydrogenation as an algorithmic process

When initiating the hydrogenation of C_{60}, the hydrogen molecule is placed in the vicinity of the selected atoms of group 1 (33 and 22 in the case illustrated by Fig. 1b), and full optimization of the complex geometry in the singlet state is performed. The shortest starting C–H distance in the first and any later calculation step was chosen to be 1.7 Å, and subsequent geometry optimization of the $C_{60}H_{2k}+H_2$ (k=1, 2, …, 29) complex which tracked down the energy minimum led to the formation of two new standard C–H bonds 1.12–1.13 Å in length. The hydrogen molecule was found to willingly attach to the cage by forming two bonds, provided that the axis of the hydrogen molecule is not normal to the chosen C–C bond. In the latter case, the molecule is repelled from the cage. Therefore, the attachment of molecular hydrogen occurs in one stage, in contrast to the two-stage molecular fluorination process [4]. Table 1 shows how the processing algorithm for C_{60} to $C_{60}H_{18}$ hydrogenation works, which is also illustrated by the Schlegel diagrams in Fig. 2.

Table 1 presents fragments of the N_{DA} Z→A lists for particular hydrides. The N_{DA} list for $C_{60}H_2$ (H2 for simplicity) points to two pairs of atoms, namely (5, 3) and (60, 57), that are depicted as light gray spheres in the $C_{60}H_2$ Schlegel diagram in Fig. 2. The atoms in each pair are connected by a short bond, thus providing two sites for the 1,2 addition of the next hydrogen molecule. Other pairs of atoms have much smaller ACS values than these first two pairs. As seen in the diagram, the bonds between 5 and 3 and 60 and 57 are not contiguous with the bond between the initial pair of atoms chosen in the algorithm, which was also the case when the algorithm was applied to the F2 fluoride [4]. The structure of the $C_{60}H_2$ molecule shown in Fig. 2 indicates that the two atom pairs marked in light gray are positionally fully equivalent. The two $C_{60}H_4$ (H4) isomers thus formed are isoenergetic, so they generate two equivalent series of successive 1,2 additions. The series that starts with the 1,2 addition involving atoms 60 and 57 will be considered below.

The N_{DA} list for H4 highlights at least four high-rank atoms. The first two atoms (31 and 34) are not linked by a short bond, and their bond partners (32 and 35, respectively)

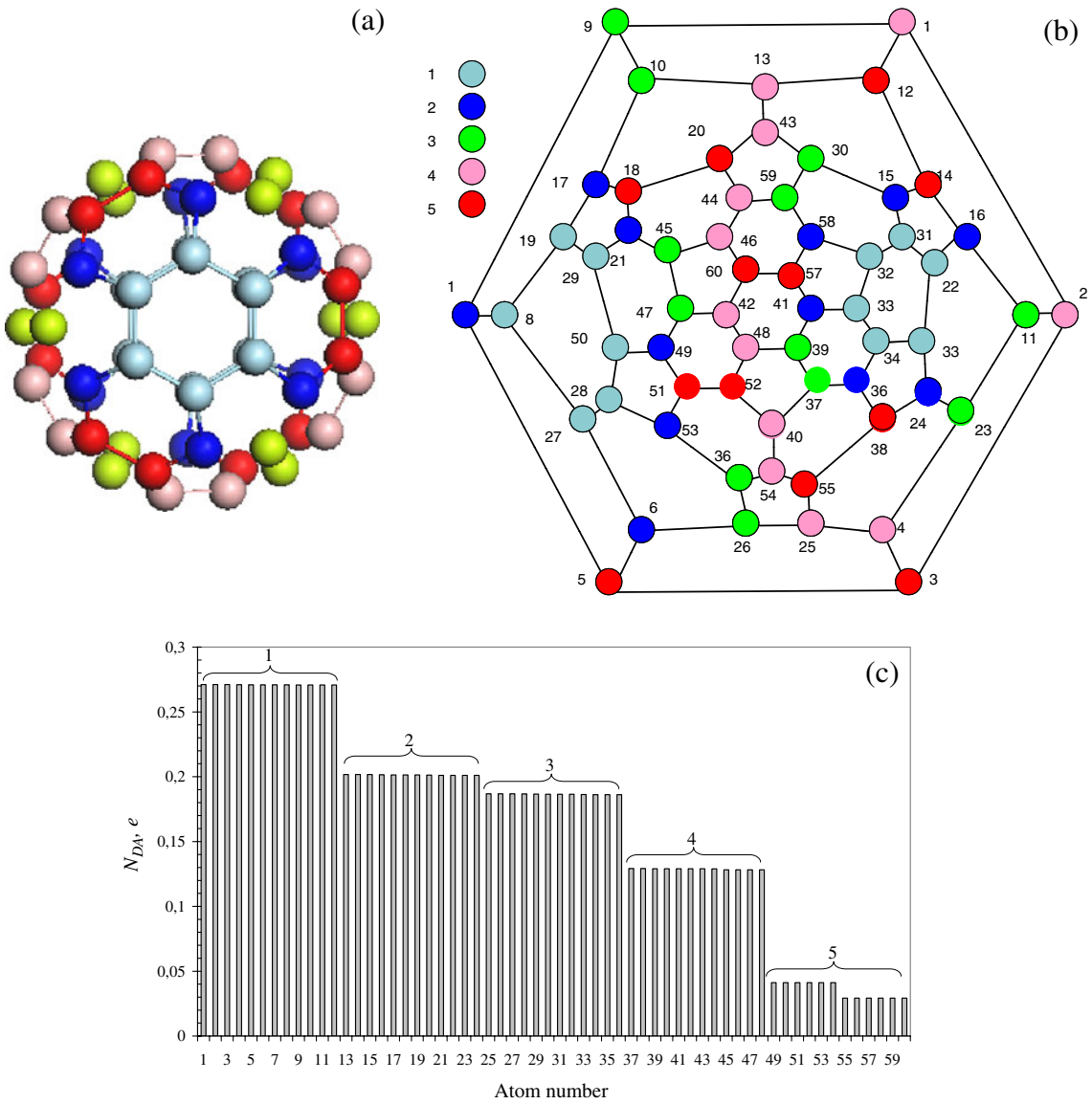

Fig. 1 **a**–**c** Chemical portrait of C_{60} [2, 3]. Colored structure of the molecule (**a**), Schlegel diagram of the molecule (**b**), and the distribution of atomic chemical susceptibility N_{DA} over the atoms of the molecule (**c**). The N_{DA} data are aligned in a Z→A manner. The colors in **a, b** correspond to the atom groups in **c**, as defined by the key in the *top left* of **b**

are located quite far down in the ACS list (a dotted line in the list in Table 1 indicates that part of the list has been removed in order to keep the table concise). Only atoms 40 and 54 form a short bond. Therefore, it is necessary to perform calculations based on (31, 32), (34, 35) and (40, 54) 1,2 additions that are aimed at finding the isomer with the least energy. As seen from the corresponding part of the table, isomer analysis based on total energy definitely favors the H6 (40, 54) isomer. Proceeding with H8 synthesis, one encounters the same situation again. The high-rank data fragment of the ACS list of H6 is headed by atoms 55 and 24, which are not bonded. Again, a set of computations for (55, 38) and (24, 23) additions need to be performed, which lead to the selection of H8 (55, 38). The same algorithm was used at each step in the synthesis, so that a series of hydrides—H10 (52, 51), H12 (31, 32), H14 (24, 23), H16 (42, 48), and finally H18 (58, 59)—was obtained. When changing from H16 to H18, there was no alternative to the combination (58, 59) according to the ACS list. The H18 hydride has a crown structure with C_{3v} symmetry, which is fully consistent with experimental findings based on ^{1}H NMR [19] and ^{3}He NMR [32] studies. Continuing the algorithmic hydrogenation, which is quite similar to fluorination [4], the higher hydrides from H20 to H60 were obtained. The structures of some of these ($C_{60}H_{36}$, $C_{60}H_{48}$, and $C_{60}H_{60}$) are given at the bottom of Fig. 2.

A series of Schlegel diagrams in Fig. 2 visualizes the chain of 1,2 additions to the C_{60} cage that result in the

Table 1 Hydrogenation algorithm in action

Atom number	NDA	Atom number	NDA	Atom number	*NDA*	Atom number	NDA	Atom number	NDA
H0-C60		H2 (22, 33)		H4 (60, 57)		H6 (40, 54)		H8 (55, 38)	
22	0.27101	5	0.29052	31	0.30726	55	0.35102	48	0.34871
33	0.27102	60	0.29051	34	0.30477	24	0.33194	52	0.33261
	…	3	0.29040	40	0.30247	31	0.29486	16	0.30018
		57	0.29039	54	0.30142	37	0.29365	12	0.28547
		42	0.26616	43	0.30044	34	0.28754	11	0.28333
		9	0.2660		…		…		…
			…	*32*	*0.25687*	23	0.27641	*51*	*0.27866*
				35	*0.25605*		…		…
					…	*38*	*0.26864*	42	0.27144
							…		…
						Isomer analysis by total energy (kcal/mol)			
						H6 (40, 54)	821.16	H8 (55, 38)	782.45
						H6 (31, 32)	830.31	H8 (24, 23)	788.56
						H6 (34, 35)	830.29		
						H6 (31, 34)	831.71		
H10 (52, 51)		H12 (31, 32)		H14 (24, 23)		H16 (42, 48)		H18 (58, 59)	
49	0.36041	24	0.40787	49	0.37686	58	0.41520	5	0.26506
31	0.35573	49	0.37738	42	0.35449	15	0.27992	4	0.26296
42	0.34512	42	0.34928	*48*	*0.34201*	46	0.27809	6	0.26036
48	0.34225	48	0.34036	29	0.29760	27	0.26521	53	0.25752
58	0.33829	29	0.30019	46	0.29412	5	0.26492	27	0.25628
	…		…	47	0.29074		…		…
47	0.28156	47	0.28866		…	*59*	*0.25405*	*3*	*0.25100*
	…		…				…		…
32	*0.27544*	*23*	*0.24824*						
	…		…						
Isomer analysis by total energy (kcal/mol)									
H10 (48, 42)	750.79	H12 (49, 47)	712.43	H14 (24, 23)	675.93	H16 (49, 47)	639.72	H18 (58, 59)	600.37
H10 (52, 51)	744. 05	H12 (31, 32)	711.31	H14 (49, 47)	678.98	H16 (42, 48)	637.59		
		H12 (42, 48)	713.14						

synthesis of the C_{60} to $C_{60}H_{18}$ hydrides step by step. As seen from the figure, the atoms do not follow a contiguous route. This behavior is also observed for higher hydrides too. As said earlier, the addition of a hydrogen molecule at each step makes the choice of 1,2 addition quite mandatory. This requirement keeps the polyene structure of the fullerene cage unchanged, which is why none of the hydrides obtained exhibits a short bond within a pentagonal structure. This conclusion is supported experimentally by the observation that the Birch reduction of C_{60}, which results in the production of $C_{60}H_{36}$, is not followed by an alteration of the fullerene skeleton [10]. In turn, this feature excludes the possibility of T_h, T, and S_6 isomers, which are characterized by short-bonded pentagonal structures in, say, $C_{60}H_{36}$ and $C_{60}H_{48}$ species. H36 and H48, as shown in Fig. 2, appear highly symmetric, while their exact symmetry is C_1. Obviously, the deviation from high symmetry is rather minor, so the products may show highly symmetric patterns in various experiments.

The geometric parameters, symmetries, and total energies of the most stable C_{60} hydrides produced through the successive attachment of hydrogen molecules to the fullerene cage are given in Table 2. This table also presents the pairs of cage atoms that participate in the 1,2 addition at each step. The hydrogenation route is very similar to that of fluorination [4], with the only difference being the cage atoms involved in the initial addition (33, 22) for hydrogenation and (32, 31) for fluorination. This finding leads to the identities of the atom pairs within group 1. In turn, the observed similarity between them strongly

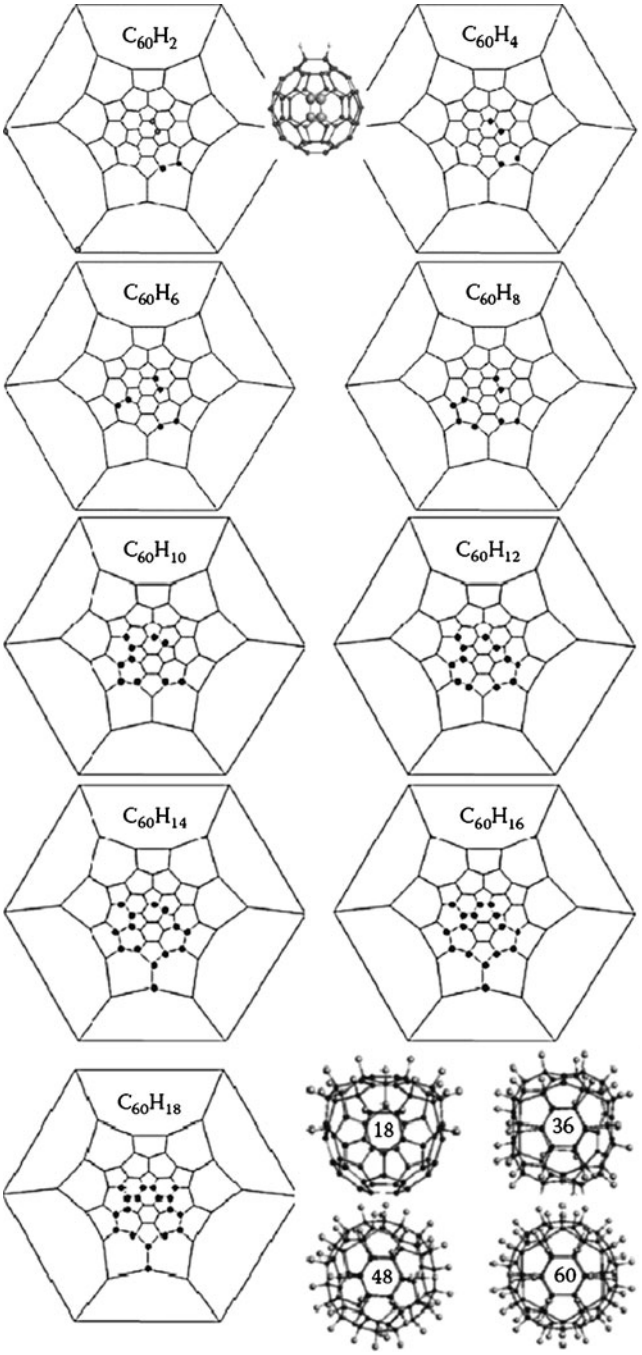

Fig. 2 Schlegel diagrams of successive hydrogenation steps from $C_{60}H_2$ to $C_{60}H_{18}$, and molecular structures of $C_{60}H_{18}$, $C_{60}H_{36}$, $C_{60}H_{48}$, and $C_{60}H_{60}$

supports the behavior of and the structural parallelism between the hydrides and fluorides of C_{60} that have been noted in numerous computational and experimental studies (see [19] and references therein).

However, when comparing similar algorithm steps for the two families, it becomes apparent that there is not a complete parallelism. While $C_{60}F_{36}$ and $C_{60}F_{48}$ were efficiently produced [33, 34], only $C_{60}H_{36}$ was obtained in significant quantities, whereas there is no mention of $C_{60}H_{48}$. The high susceptibility of C_{60} hydrides to oxidation is one of the reasons why it is difficult to stabilize and efficiently produce high hydrides. Another is intimately related to the different efficacies of the hydrogenation and fluorination processes.

Comparison of the efficacies of fluorination and hydrogenation reactions

Leaving aside kinetic parameters (which are undoubtedly very important when performing the reaction in practice), let us now concentrate on static parameters. We will consider the evolution of the total ΔH and the coupling energies E_{cpl} of the products, as well as their molecular chemical activities N_{D}, as a function of the pair number k. The quantity E_{cpl} determines the energy that is needed to add each pair of either hydrogen or fluorine atoms to the fullerene cage. Assuming that the reaction occurs in molecular gas, the coupling energy is determined as

$$E_{\mathrm{cpl}} = \Delta H_{2k} - \Delta H_{2(k-1)} - \Delta H_{\mathrm{mol}}. \quad (1)$$

Here ΔH_{2k} and $\Delta H_{2(k-1)}$ are the heats of formation of the H2k and H2(k−1) products, while ΔH_{mol} is the heat of formation of either the fluorine or the hydrogen molecule (−22.38 kcal mol^{-1} and −5.18 kcal mol^{-1}, respectively). For k=1, E_{cpl} is −86.3 and −40.62 kcal mol^{-1} for F2 and H2, respectively, demonstrating how tightly both molecules bind to the fullerene cage.

Figure 3 presents the evolutions of ΔH, E_{cpl} and N_{D} during hydrogenation and fluorination. As seen from the figure, the two reactions are characterized by significantly different energetic parameters, with fluorination clearly favored in terms of both ΔH and E_{cpl}. Actually, the total energy ΔH of the hydrides gradually decreases, which favors polyhydride formation, until k reaches 25, after which this decrease slows down and then the total energy starts to increase slightly. The coupling energy E_{cpl} is negative until k reaches 25 (excluding k=22) but becomes steadily positive at k>25. The total and the coupling energies of fluorides show similar behaviors, with the only differences being the larger change in ΔH and the greater absolute magnitude of E_{cpl}, as well as the absence of an increase in ΔH at k >25.

The molecular chemical susceptibility N_{D} is the other characteristic quantifier. This quantity is shown in the top part of Fig. 3b. As seen in the figure, the $N_{\mathrm{D}}(k)$ functions are practically identical for both families; they gradually decrease at higher k and approach zero at k~20–24. Therefore, a decreasing absolute value of E_{cpl} correlates with decreasing molecular chemical susceptibility N_{D}; in other words, the pool of effectively unpaired electrons becomes used up, which results in a considerable drop in

Table 2 Geometric parameters, symmetries, and total energies of hydrogenated C_{60} fullerenes (AM1 UBS HF)

	H2	H4	H 6	H 8	H10	H 12	H 14	H 16	H 18	H 20
R(C*–H)[a] (Å)	1.126	1.126	1.126–1.129	1.126–1.130	1.126–1.130	1.126–1.129	1.125–1.131	1.126–1.130	1.126–1.130	1.126–1.130
R(C*–C*)[b] (Å)	1.55	1.55–1.52	1.54–1.50	1.54–1.50	1.54–1.50	1.54–1.50	1.54–1.50	1.54–1.50	1.54–1.50	1.54–1.50
ΔH[d] (kcal/mol)	909.57	862.22	821.16	788.56	744.05	711.31	675.93	637.59	600.31	561.95
Symmetry	*C*v	*C*s	*C*1	*C*1	*C*1	*C*1	*C*1	*C*s	*C*3v	*C*1
Atom pair	*22, 33*	*60, 57*	*40, 54*	*55, 38*	*52, 51*	*31, 32*	*24, 23*	*42, 48*	*58, 59*	*5, 3*
	H 22	H 24	H 26	H 28	H 30	H 32	H 34	H 36	H 38	H 40
R(C*.F)[a] (Å)	1.126–1.131	1.126.1.133	1.126–1.133	1.126–1.133	1.126–1.135	1.126–1.135	1.127–1.135	1.128–1.135	1.127–1.140	1.127–1.140
R(C*.C*)[b] (Å)	1.54–1.50	1.58–1.50	1.54–1.50	1.54–1.50	1.57–1.50	1.57–1.50	1.57–1.50	1.57–1.50	1.57–1.50	1.57–1.49
ΔH[d]. kcal/mol	530.03	499.37	460.93	428.56	394.43	369.60	343.06	321.72	301.07	290.98
Symmetry	*C*1	*C*s	*C*s	*C*1	*C*1	*C*1	*C*s	*C*1	*C*1	*C*1
Atom pair	*6, 26*	*27, 28*	*13, 43*	*10, 17*	*8, 19*	*1, 2*	*12, 14*	*47, 49*	*50, 29*	*20, 18*
	H 42	H 44	H 46	H 48	H 50	H 52	H 54	H 56	H 58	H 60
R(C*.F)[a] (Å)	1.128–1.140	1.129–1.139	1.130–1.141	1.132–1.141	1.133–1.146	1.133–1.146	1.132–1.146	1.138–1.146	1.138–1.146	1.146 (1.112)
R(C*–C*)[b] (Å)	1.57–1.49	1.57–1.50	1.57–1.49	1.56–1.48	1.55–1.48	1.55–1.49	1.55–1.48	1.54–1.49	1.53–1.50	1.53–1.50
ΔH[c] (kcal/mol)	273.93	270.67	253.28	255.06	256.98	272.49	287.98	303.45	318.82	334.16
Symmetry	*C*1	*C*1	*C*s	*C*1	*C*2v	*C*s	*C*2v	*C*2h	*C*2v	*I*h
Atom pair	*44, 46*	*35, 34*	*36, 37*	*25, 4*	*11, 16*	*53, 56*	*15, 30*	*21, 45*	*39, 41*	*7, 9*

[a] C* indicates the cage atom to which hydrogen is added

[b] C*–C* indicates a new short bond to the cage through which a pair of hydrogen atoms is added

[c] ΔH is the heat of formation, determined as $\Delta H = E_{\text{tot}} - \sum \left(E^{A}_{\text{elec}} + EHEAT^{\text{A}}\right)$. Here $E_{\text{tot}} = E_{\text{elec}} + E_{\text{nuc}}$, while $E_{\text{elec}}$and E_{nuc} are the electron and core energies. E^{A}_{elec} and $EHEAT^{A}$ are the electron energy and the heat of formation of an isolated atom, respectively

reactivity when k changes from 18–20 to 25–26. According to both characteristics, the reaction terminates at k >25. It is important to note that, in spite of the obvious obstacles to their creation, high-k products can still be found among the final products. This is due to the accumulative character of the reaction while the next atom-pair addition is still energetically favorable, which means that (i) the attachment of another atom pair will not proceed at positive E_{cpl}, and (ii) the accumulation time (and the mass yield of the product) will greatly depend on the absolute value of E_{cpl}: the lower the value, the longer the time needed. This is why the absolute E_{cpl} values for hydrides are four times less than those of fluorides at k=18, and these smaller absolute values result in the termination of the hydrogenation process at the $C_{60}H_{36}$ product while fluorination continues until $C_{60}F_{48}$.

Transformation of the C_{60} cage structure during hydrogenation

Stepwise hydrogenation results in the gradual substitution of sp^2-configured carbon atoms for sp^3 ones. Since both the valence angles and the corresponding C–C bond lengths are noticeably different for these two configurations, the structure of the fullerene cage becomes markedly distorted. Figure 4 demonstrates the transformation of the cage structure during hydrogenation through the changes to a fixed set of C–C bonds.

The gray line in each panel in Fig. 4 represents the bond length distribution for the pristine C_{60} fullerene molecule. It is apparent that the first hydrogenation steps are followed by the elongation of C–C bonds that involve not only newly formed sp^3 atoms but also some sp^2 atoms. This results in a noticeable growth in the total number of effectively unpaired electrons N_{D} (see [3]). A detailed comparison of this effect for hydrides and fluorides is presented in Fig. 5. As seen from the figure, the two families show generally similar behavior, which is one more manifestation of the parallelism of fluorination and hydrogenation. The growth in N_{D} proceeds until six additions have occurred, after which the former effect is compensated for by a gradual decrease in the N_{D} value due to the increasing number of sp^3 atoms. However, the two curves differ slightly, and, as expected, they differ in terms of the influence of the species attached to the fullerene cage.

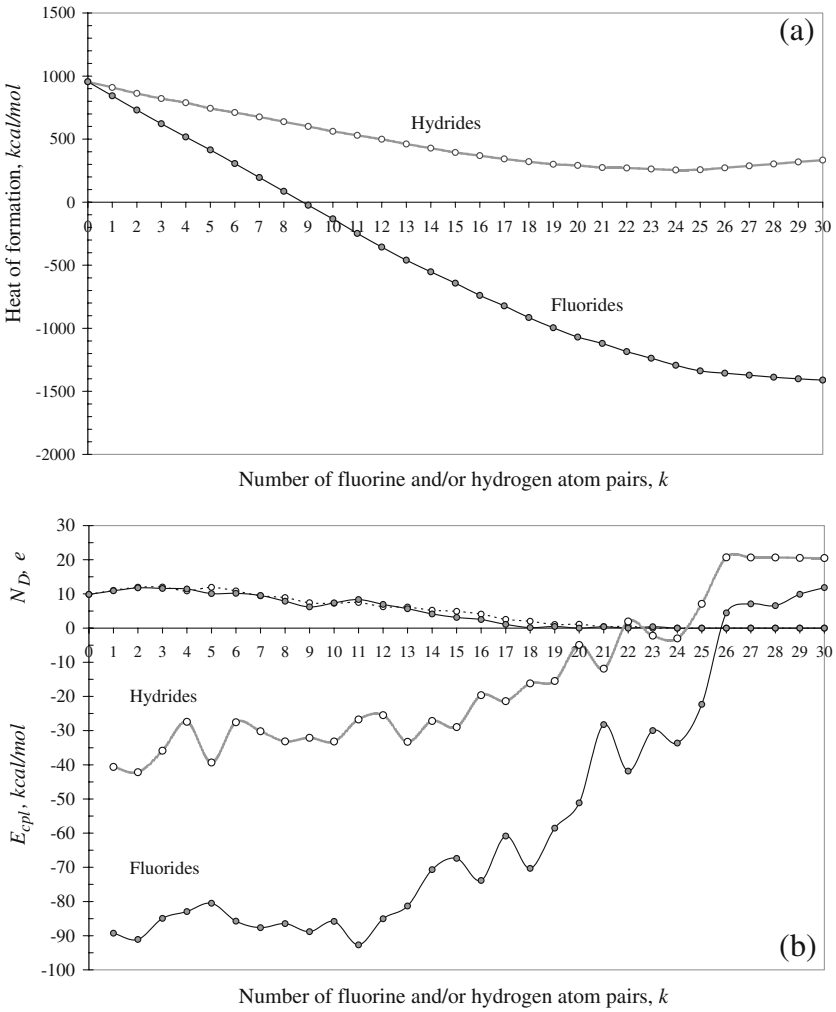

Fig. 3 **a**–**b** Evolutions of the total energy (**a**), N_D and the coupling energy E_{cpl} (**b**) with number of atom pairs k for C_{60} hydrides (*dotted curves with empty circles*) and C_{60} fluorides (*solid curves with filled circles*)

Comparing the bond length distribution for the pristine C_{60} fullerene molecule with the corresponding distributions for different hydrides in Fig. 4 makes it possible to trace the changes in the fullerene cage structure as the hydrogenation process progresses. As might naturally be expected, the sp^2–sp^3 transformation causes the appearance of elongated C–C bonds, which increase in number as hydrogenation proceeds. To keep the cage structure closed, this effect, as well as changes in valence angles, needs to be compensated for. At the bond level, this compensation involves shortening many of the pristine bonds, both long and short. Long bonds connected to empty sites become shorter and shorter until they reach 1.395 Å; below this bond length, complete covalent bonding of the remaining odd electrons occurs [3]. This causes the number of effectively unpaired electrons N_D to approach zero at k~20–24, well before all of the empty sites have been occupied by hydrogen atoms. This "squeezing effect" is particularly apparent in the right-hand panels of Fig. 4, which relate to high-k hydrides; here, a number of extremely short (1.325–1.320 Å) C–C bonds are observed. These six bonds are the only ones that remain unsaturated in $C_{60}H_{48}$ species and provide information about the pristine structure. Once each of them has been saturated (i.e., following hydrogenation from $C_{60}H_{48}$ to $C_{60}H_{60}$), a new unstressed cage of I_h symmetry is formed. It is important to note that in spite of the fact that all of the carbon atoms become sp^3-configured and should be considered identical, the short-and-long bond pattern of the pristine C_{60} is also maintained for $C_{60}H_{60}$. Moreover, bonds that were previously short or long in C_{60} keep their character in $C_{60}H_{60}$, thus supporting the stability of the fullerene skeleton's polyene structure. Observing this stability at both ends of the hydrogenation cycle, it is difficult to suggest its violation somewhere inside the cycle. This means that highly symmetric structures should not be expected for high-k species, so the C_{3v}–$C_{60}H_{18}$ is the only high-symmetry structure that is allowed for the polyene structure of the C_{60} skeleton. The discussion provided above also applies to the sp^2–sp^3 transformation of the cage under fluorination from C_{60} to $C_{60}F_{60}$ [4]; the structural parallelism between the two families is deeply routed in the tendency of the fullerene skeleton to retain its structure if possible.

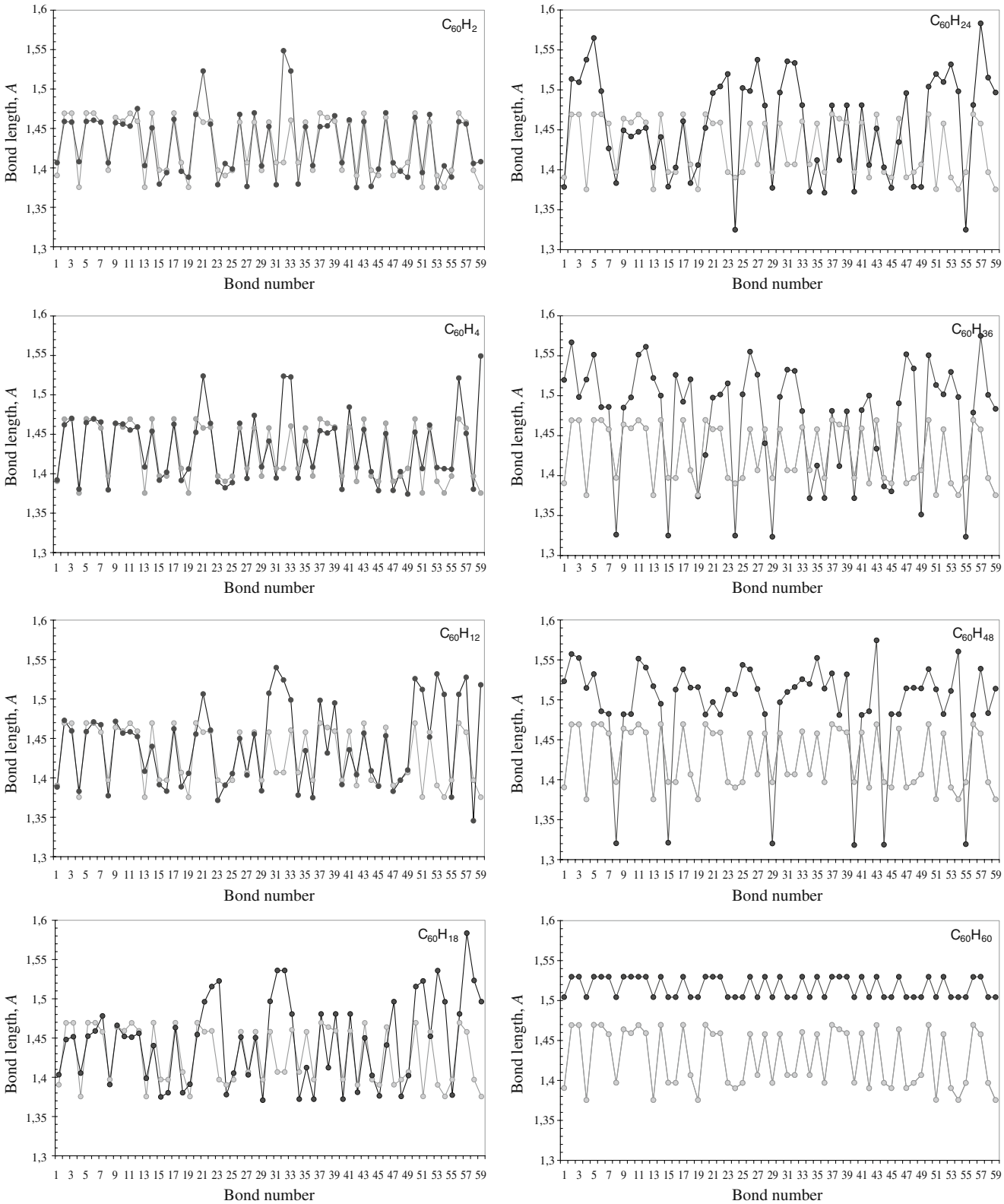

Fig. 4 sp^2–sp^3 transformation of the C_{60} cage structure through successive hydrogenation. *Gray* and *black lines* correspond to the bond length distributions of the pristine C_{60} fullerene cage and the C_{60} fullerene hydride cage, respectively

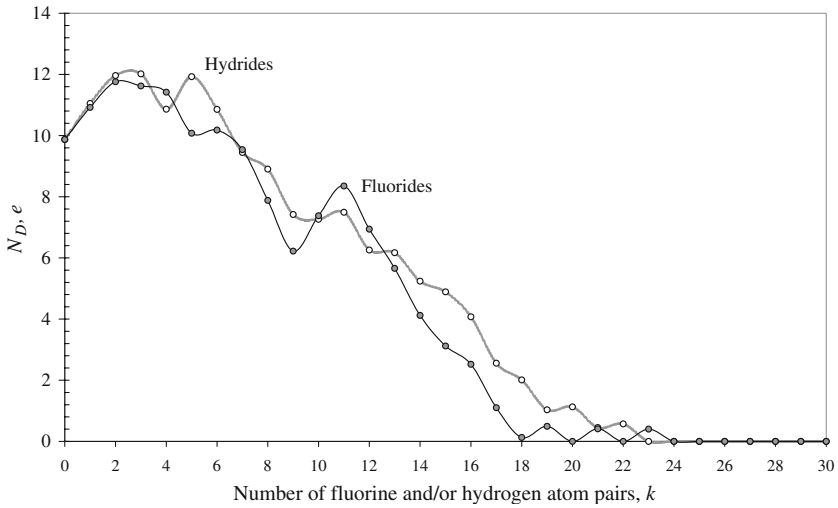

Fig. 5 Molecular chemical susceptibility versus number of atom pairs for C_{60} hydrides (*dotted curves with empty circles*) and C_{60} fluorides (*solid curves with filled circles*)

Comparison with experiments

C_{60} hydride chemistry offers two main issues that need to be explained computationally. The first concerns the path of the hydrogenation reaction, and covers such key points as the production of a limited number of different hydrides (the main products $C_{60}H_{18}$ and $C_{60}H_{36}$, plus the di- and tetrahydroderivatives only) [35], the termination of C_{60} hydrogenation at $C_{60}H_{36}$, and the amount of product produced. Any reaction is under the control of a complex set of static and kinetic conditions. Some arguments that may be useful for solving the problem from the static viewpoint were discussed in the previous section. They evidently allow hydrogenation and fluorination processes to be distinguished at a semiquantitative level at the very least.

The second issue concerns the structural composition of the product in view of the difficult manyfold isomerism problem. A lot of experimental and computational effort has been expounded to solve this problem for $C_{60}H_{18}$ and $C_{60}H_{36}$. Experimentally, these two hydrides behave quite differently: the former is mainly observed as a monoisomer, while the latter is usually present as a mixture of isomers [10, 19]. Moreover, the isomer composition in the latter case depends on the synthetic route, and can include from one to five components [10]. The $C_{60}F_{18}$ fluoride is also monoisomeric [36], while $C_{60}F_{36}$ is produced as two isomers [37].

A chemical reaction generally produces a number of different isomers when there is only a small difference in the total energies of the components. Supposing that the output hydrides are formed during the successive attachment of hydrogen molecules to the fullerene cage, and that all of the isomers of each hydride contain the same species, the isomer families of $C_{60}H_{18}$ or $C_{60}H_{36}$ can be considered a set of products that are generated according to the N_{DA} lists for the relevant precursors H16 and H34. Table 3 presents isomer families for the hydrides H18 and H36, as generated from the best H16 and H34 precursors given in Table 2. The table contains N_{DA} lists for both precursors, along with the number of atoms associated with each value of N_{DA}, the atom pairs that participate in the formation of the H18 and H36 isomers, and their total energies. Isomer symmetries are shown in parentheses. The tables shows that H18 should really be a monoisomeric product, as the smallest energy difference $\delta(\Delta H)$ between the C_{3v} product with the lowest ΔH and any other member of the set is quite large; at least 2.3 kcal mol^{-1}. The situation for the second hydride is drastically different. The smallest energy difference $\delta(\Delta H)$ is 0.6 kcal mol^{-1}, and the largest does not exceed 1.1 kcal mol^{-1}, which means that there will be competition in terms of the isomers produced. Evidently, the five isomers that start the list should be considered the main candidates for the product. They all are nonsymmetric (C_1), so that experimental results for different sets of isomers should share a lot of similarities, which is actually observed in practice [10].

The situation with the fluorides F18 and F36 is different. The smallest $\delta(\Delta H)$ values, obtained using an analysis similar to that discussed above, are 6.2 and 4.2 kcal mol^{-1} for F18 and F36, respectively. Both quantities strongly support a monoisomeric regime. The two-isomer output of $C_{60}F_{36}$ may be connected to the particular experimental conditions used to generate the product [36], which greatly stimulate the kinetic component of the reaction. Concluding, it should be noted that the difference in the energetic parameters of hydrides and fluorides not only governs their different reaction paths, which manifest themselves as different conditions for reaction termination, but also influences the isomeric compositions of the reaction products.

There is no disagreement between the experimental and computational communities in attributing exact C_{3v} sym-

Table 3 Comparative energetics of H18 and H36 isomers

	H16		H18		H34		H36
N	NDA	Atom pair	ΔH (kcal/mol)	*N*	NDA	Atom pair	ΔH (kcal/mol)
58	0.41520	58, 59 (C_{3v})	600.307	47	0.21499	47,49 (C_1)	322.688
15	0.27992	15,3O (C_1)	602.604	46	0.21429	44,46 (C_1)	323.743
46	0.27809	46, 47 (C_1)	602.612	29	0.21407	29,5O (C_1)	323.270
27	0.26521	27, 28 (C_1)	603.657	18	0.21373	18,2O (C_1)	323.723
5	0.26492	3,5 (C_1)	603.673	49	0.20339	21,45 (C_s)	323.765
				44	0.20286		
				50	0.20197		
				20	0.20179		
				21	0.17842		
				45	0.17785		
				39	0.07026		
				41	0.07014		

metry to the monoisomeric $C_{60}H_{18}$ hydride. For $C_{60}H_{36}$, data obtained from structure-sensitive experimental techniques such as ^1H, ^{13}C, and ^3He NMR are rather complicated and not sufficiently fine-structured, which results in ambiguity during molecular symmetry determination. This is why references to T_h, T, S_6, D_{3d}, C_3, and C_1 can all be found in the available literature (for a comprehensive review, see [10]). Computationally, numerous attempts have been made to select the best candidate for the isomeric structure. In these works, the choice between T_h, T, S_6, D_{3d}, C_3, and C_1 representatives was made using different computational techniques and by guessing the appropriate structure within each symmetric group. The only approach that has a predictive capacity and does not need to be applied to a structure with a particular symmetry is suggested in the present paper.

According to the algorithm for determining the sites at which hydrogen molecules are successively attached to the fullerene cage, stepwise hydrogenation from C_{60} to $C_{60}H_{18}$ results in the formation of the C_{3v}-H18 hydride, in full accordance with experimental data. The close similarity of this stage of hydride synthesis to the corresponding one for fluorides suggests that this pattern is connected to the particular algorithmic response of the fullerene skeleton's electronic structure to stepwise attachment of molecules in the absence of steric hindrance due to obstacles. As has recently been shown, this expectation was confirmed by the results of a similar computational synthesis of C_{60} to $C_{60}(CN)_{18}$ and $C_{60}(NH)_9$ derivatives [38].

Two main results follow from the application of the algorithm to $C_{60}H_{36}$:

(1) C_{60} to $C_{60}H_{36}$ hydrogenation (involving a C_{60} to $C_{60}H_{18}$ stage) is achieved by successive 1,2 additions, which allows the polyene structure of the fullerene skeleton to be maintained. The conservation of this structure means that we can exclude from our considerations H36 isomers with symmetries that imply the presence of a pentagonal structure containing a double bond, such as T_h, T, S_6, D_{3d}, C_3, etc. At the same time, the approach logically completes the $C_{60}H_{2k}$ series by producing a single $C_{60}H_{60}$ isomer of I_h symmetry, as discussed in the previous section.

(2) Within the framework of the approach, the best isomer, H36 (structure given in Fig. 2), is nonsymmetric (C_1). Despite its exact symmetry status, the molecule appears to be quite symmetrical, so we can expect a significant contribution from a high-symmetry pattern in experimental data. Alongside the multi-isomer character of the product discussed earlier, this may provide a reasonable explanation of the empirical results.

Conclusions

The reaction of fullerene C_{60} with molecular hydrogen was studied in the framework of an unrestricted broken symmetry HF SCF semiempirical approach (UBS HF version of the AM1 technique of the CLUSTER-Z1 codes). The calculations focused on successive 1,2 additions of hydrogen molecules to the fullerene cage. A complete family of species of formula $C_{60}H_{2k}$ (k=1, ..., 30) was computationally synthesized. Based on the effectively unpaired electron concept for the atomic chemical susceptibility, as well as a suggested methodology for the computational synthesis of fullerene derivatives [2, 3], the synthesis of hydrides was performed as a series of predicted steps. The preferred binding sites for the series of 1,2 additions were selected according to the largest value of the atomic chemical susceptibility, as quantified by the effectively unpaired electron fraction N_{DA} for each atom, which was calculated at each step. This approach circumvented

the difficulties due to the manyfold isomerism problem associated with these fullerene species, and released the computational scheme from both the need to use a contiguous approach to sequential addition and the need to look for high-symmetry models for high-k hydrides ($k \geq 9$). By searching for the isomer with the lowest total energy, the synthetic methodology described in the present work identifies the isomers generated for $C_{60}H_{2k}$ (k=1, ..., 30) species. The results obtained reveal that there is a structural parallelism between C_{60} hydrogenates and C_{60} fluorinates that arises from a tendency to retain the polyene structure of the fullerene skeleton. However, the much weaker interactions of hydrogen molecules with the fullerene cage in comparison with those of fluorine molecules cause a significant difference in the species produced, as hydrogenation terminates at $C_{60}H_{36}$ while $C_{60}F_{48}$ is the most abundant of the fluorides produced.

References

1. Sheka EF (2004) Int J Quantum Chem 100:375–387
2. Sheka EF, Zayets VA (2005) Russ J Phys Chem 79:2009–2014
3. Sheka EF (2007) Int J Quantum Chem 107:2803–2816
4. Sheka EF (2010) J Exp Theor Phys 111:395–412
5. Balasubramania K (1991) Chem Phys Lett 182:257–262
6. Book LD, Scuseria GE (1994) J Phys Chem 98:4283–4286
7. Dunlap BI, Brenner DW, Schriver GW (1994) J Phys Chem 98:1756–1757
8. Bühl M, Tiel W, Schneider U (1995) J Am Chem Soc 117:4623–4627
9. Cahill PA, Rohlfing CM (1996) Tetrahedron 52:5247–5256
10. Nossal J, Saini RK, Sadana AK, Bettinger HF, Alemany LB, Scuseria GE, Billups WE, Saunders M, Khong A, Weisemann R (2001) J Am Chem Soc 123:8482–8495
11. Clare BW, Kepert DL (1993) J Mol Struct THEOCHEM 281:45–52
12. Clare BW, Kepert DL (1994) J Mol Struct THEOCHEM 303:1–9
13. Clare BW, Kepert DL (1994) J Mol Struct THEOCHEM 304:181–189
14. Clare BW, Kepert DL (1994) J Mol Struct THEOCHEM 315:71–83
15. Clare BW, Kepert DL (1996) J Mol Struct THEOCHEM 363:179–190
16. Clare BW, Kepert DL (2002) J Mol Struct THEOCHEM 589–590:195–207
17. Clare BW, Kepert DL (2002) J Mol Struct THEOCHEM 589–590:209–227
18. Darwish AD, Avent AG, Taylor R, Walton DRM (1996) J Chem Soc Perkin Trans 2:2051–2054
19. Boltalina OV, Bühl M, Khong A, Saunders M, Street JM, Taylor R (1999) J Chem Soc Perkin Trans 2:1475–1479
20. Haufer RE, Conceicao, Chibante LPF, Chai Y, Byrne NE, Flanagan S, Haley MM, O'Brien SC, Pan C, Xiao Z, Billups WE, Ciufolini MA, Hauge RH, Margrave JL, Wilson LJ, Curl RF, Smalley RE (1990) J Phys Chem 94:8634–8636
21. Rüchardt C, Gerst M, Ebenhoch J, Beckhaus HD, Cambell EEB, Tellgmann R, Schwarz H, Weiske T, Pittes S (1993) Angew Chem Int Ed Engl 32:584–586
22. Attalla MI, Vassallo AM, Tattam BN, Hanna JV (1993) J Phys Chem 97:6329–6331
23. Matsuzawa N, Fukunaga T, Dixon DA (1992) J Phys Chem 96:10747–10756
24. Noodleman L (1981) J Chem Phys 74:5737–5742
25. Takatsuka K, Fueno T, Yamaguchi K (1978) Theor Chim Act 48:175–183
26. Staroverov VN, Davidson ER (2000) Chem Phys Lett 330:161–168
27. Kaplan I (2007) Int J Quantum Chem 107:2595–2603
28. Sheka EF, Chernozatonskii LA (2010) Int J Quantum Chem 110:1466–1480
29. Noodleman L, Davidson E (1986) Chem Phys 109:131–143
30. Han WC, Noodelman L (2008) Inorg Chim Acta 361:973–986
31. Saunders M (1991) Science 253:330–331
32. Darwish AD, Abdul-Sada AK, Langley GJ, Kroto HW, Taylor R, Walton DRM (1995) J Chem Soc Perkin Trans 2:2359–2366
33. Taylor R (2001) Chem Eur J 7:4074–4084
34. Taylor R (2004) J Fluorine Chem 125:359–368
35. Avent AG, Darwish AD, Heimbach DK, Kroto HW, Meidine MF, Parsons JP, Remars C, Roers R, Ohashi O, Taylor R, Walton DRM (1994) J Chem Soc Perkin Trans 2:15–22
36. Boltalina OV, Markov V, Yu, Taylor R, Waugh MP (1996) Chem Commun 2549–2550
37. Boltalina OV, Street JM, Taylor R (1998) J Chem Soc Perkin Trans 2:649–653
38. Sheka EF (2010) Nanochemistry of fullerene C_{60} Cyano- and azopolyderivatives. arXiv:10074089v1